ISSN 1345-3041

Mar.2020 / Vol.169

Mitsubishi Electric

ADVANCE

Advanced Technologies of Automotive Equipment to Create Future of Mobility

MITSUBISHI ELECTRIC
Changes for the Better

Mar. 2020 / Vol. 169
Mitsubishi Electric
ADVANCE
Advanced Technologies of Automotive Equipment to Create Future of Mobility

• **Editorial Inquiries**
Tomoyuki Kobayashi
Corporate Total Productivity Management
& Environmental Programs
Fax: +81-3-3218-2465

Mitsubishi Electric Advance is published on line quarterly (in March, June, September, and December) by Mitsubishi Electric Corporation.

CONTENTS

Technical Reports

Precis

Currently, it is said that, with a situation surrounding automobiles that is significantly changing due to autonomous driving and motorization, the automobile industry is undergoing an evolution the likes of which haven't been seen for 100 years. This special issue aims to shine a spotlight on this situation, along with the state-of-the-art technologies used in our onboard equipment and systems, all aiming to solve problems amid this current situation and to contribute to an ever-better society of mobility.

Overview

Author: *Hiroshi Onishi**

Special Issue on Advanced Technologies for Automotive Devices for the Future of Mobility

The auto industry is facing a paradigm shift involving autonomous driving and motorization.

Autonomous driving is being developed to improve convenience and reduce the number of casualties in traffic accidents. Systems that use cameras and onboard sensors such as radar to recognize the situation around automobiles and assist driving have been spreading; these include braking systems to reduce collision damage and systems to assist lane-keeping. Mitsubishi Electric Corporation provides advanced driving support by combining such self-sensing autonomous driving technologies with infrastructure-linked traveling technologies, using signals from quasi-zenith satellite systems and highly accurate maps.

CO2 emissions from vehicles are being reduced to help curb global warming, since CO2 emissions from automobiles account for 20% of total emissions. Various countries, particularly in Europe, have been tightening emissions controls and penalties. This is boosting the use of hybrid vehicles in which the engine is combined with electric power, as well as all-electric vehicles. Mitsubishi Electric has been contributing to this trend by supplying on-board power semiconductor devices, applying them to power electronics, downsizing drive systems that include motors, and improving their efficiency.

This special issue introduces our technologies and related new products.

**Group President, Automotive Equipment*

Development and Experiment of ADAS and Autonomous Driving System

Authors: *Fumiaki Kadoya** and *Kazuo Hitosugi**

To realize autonomous driving, technologies for determining the position of one's own vehicle and information on the surroundings with high accuracy are required. Mitsubishi Electric Corporation has developed an autonomous driving system and verified its feasibility in demonstration experiments on public roads. In this system, self-sensing technologies using onboard sensors (e.g., cameras and radar) are combined with infrastructure-linked technologies utilizing infrastructure such as artificial satellites and intelligent transportation systems.

1. Definition of levels of driving automation

Autonomous driving is divided into various levels depending on the extent to which drivers are involved and operations that the system performs. The research and development plan for autonomous driving systems under the Cross-Ministerial Strategic Innovation Promotion Program (SIP) led by the Japanese Cabinet Office adopted J3016 (U.S.) (September 2016) of the Society of Automotive Engineers (SAE) as the definitions of the levels of driving automation (Table 1). In addition, the program aims to commercialize SAE Level 3 in 2020 and SAE Level 4 in 2025.

2. Utilization of quasi-zenith satellite system

To establish the infrastructure-linked autonomous driving system, the centimeter level augmentation service (CLAS) of the quasi-zenith satellite system (QZSS) was used. Formal operation of the QZSS in Japan began in November 2018. The system has a supplement function that sends positioning signals

Table 1 Definitions of Autonomous Driving Level

Level	Outline	Entity that performs monitoring and operation for safety driving
The driver performs all or some driving tasks.		
SAE Level 0 No automation	• The driver performs all driving tasks.	Driver
SAE Level 1 Driver assistance	• The system performs sub-tasks of driving tasks for vehicle control of any of the front, rear and sides.	Driver
SAE Level 2 Partial automation	• The system performs sub-tasks of driving tasks for vehicle control of both the front and rear and sides.	Driver
The autonomous driving system performs all driving tasks.		
SAE Level 3 Conditional automation	• The system performs all driving tasks (within a limited range*). • When continuous operation is difficult, the driver is expected to respond appropriately to a system request to intervene.	System (When continuous operation is difficult, the driver)
SAE Level 4 High automation	• The system performs all driving tasks (within a limited range*). • When continuous operation is difficult, the user is not expected to respond.	System
SAE Level 5 Full automation	• The system performs all driving tasks (not within a limited range). • When continuous operation is difficult, the user is not expected to respond.	System

Note: The term "range" is not limited to a geographical area and includes environmental, traffic condition, speed, and temporal factors.

Source: Research and development plan 2018 for autonomous driving systems in the Cross-Ministerial Strategic Innovation Promotion Program under the Japanese Cabinet Office

**Automotive Electronics Development Center*

compatible with the GPS of the U.S. and an augmentation function that sends augmentation signals for improving the positioning accuracy within Japan. Conventional satellite positioning uses positioning signals from global navigation satellite systems (GNSSs) such as GPS. Such positioning includes errors of the satellites (errors of satellite orbit, satellite clock, and satellite signal bias) and errors due to positioning areas (ionospheric delay and tropospheric delay errors). Positioning errors are in the order of several meters. The CLAS uses the electronic reference point network provided by the Geospatial Information Authority of Japan to create augmentation signals to correct errors for each satellite and area and sends them via the QZSS to improve the positioning accuracy with errors in the order of centimeters (Fig. 1).

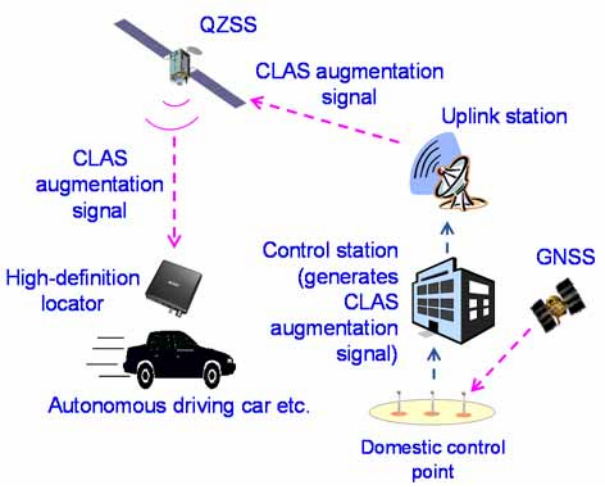

Fig. 1 Centimeter Level Augmentation Service

Four companies including Mitsubishi Electric have established Sapcorda Services GmbH to provide high-accuracy positioning services that allow satellite positioning with centimeter order also outside Japan. These services make it possible to use satellite augmentation signals that are compatible with the CLAS and to establish the infrastructure-linked autonomous driving system outside Japan.

3. Infrastructure-linked autonomous driving system

When a GNSS is used to estimate the position of a vehicle, the absolute position is expected to be highly accurate. However, signals may be blocked by obstacles on the road and the output of the satellite signals may be delayed. Mitsubishi Electric has developed GNSS/INS (autonomous navigation system) compound navigation in which the vehicle state obtained by the inertial sensor is used to compensate the satellite positioning signals in order to handle interruptions of satellite signals and output delays.

It has been verified that the combination of high-accuracy vehicle position estimation technologies based on GNSS/INS compound navigation with high-definition 3D maps, which are called dynamic maps, makes it possible to identify the self-positions of vehicles in lanes on expressways. To date, Mitsubishi Electric has developed high-accuracy lane-keeping and autonomous lane change systems for expressways by combining high-accuracy identification of the self-positions of vehicles with information provided from the roadside and nearby vehicles. Examples of assistance operations expected in the future are the creation of routes to target destinations (target exit ramps) for which even the lanes are selected, and application to autonomous driving when vehicles merge with and leave other traffic.

In addition, Mitsubishi Electric has been working to expand the use of high-accuracy positional information services around the world in cooperation with Here Technologies. We are working to provide smooth guidance on a recommended lane in case of an accident and traffic congestion through high-accuracy positioning in real time by combining high-definition maps and high-accuracy satellite positioning technologies with cloud positional information services.

4. Self-sensing autonomous driving system

The driving functions of vehicles are broadly divided into recognition, judgment, and manipulation. When a human driver drives a vehicle, the driver recognizes the road environment, traffic signals, pedestrians, and other factors in front of the vehicle from perceptual information, judges with the brain to what extent the steering wheel and other components need to be manipulated, and uses the hands and feet to manipulate the vehicle's devices. The aforementioned satellite positioning system is equivalent to the recognition function in autonomous driving.

As self-sensing devices to handle the recognition function, Mitsubishi Electric has been developing technologies such as millimeter wave radar (object identification function), forward-looking cameras, vehicle periphery monitoring cameras, ultrasonic sensors, and driver monitors. By combining information from such self-sensing devices, electric power steering (EPS) control technologies, and advanced driving assistance system-ECU (ADAS-ECU), a sophisticated driving assistance system that leads to autonomous driving technologies has been developed. Examples of such technologies are autonomous emergency braking to avoid collision with a pedestrian in front of the vehicle, lane-keeping system, adaptive cruise control system, and autonomous parking system. In addition to these systems, we are developing human machine interface (HMI) systems that notify the states of the autonomous driving systems to the occupants while traveling.

5. Vehicle control system

Mitsubishi Electric developed the xAUTO autonomous driving demonstration vehicle that has infrastructure-linked and self-sensing autonomous driving systems and verified the feasibility of the autonomous driving system through experiments on public roads. The vehicle control system on xAUTO consists of the three functions of the sensor section, locator section, and ADAS-ECU (Fig. 2).

The sensor sections refer to self-sensing devices such as a QZSS antenna, inertial sensor, forward-looking camera, and millimeter wave radar. The locator section accurately estimates the self-position of the vehicle on the map by combining high-precision position calculation by satellite positioning, vehicle state, shape of the road (white line), and high-definition 3D maps provided in the system; and outputs positional information on the vehicle, target route, and information on surrounding roads (e.g., speed limit). The ADAS-ECU calculates control amounts (e.g., steering amount, acceleration amount, and braking amount) for various driving assistance systems based on the information from the locator section, vehicle state, and other information and issues commands to the actuators on the vehicle. In addition, the ADAS-ECU ensures mutual cooperation between the infrastructure-linked autonomous driving system and the self-sensing autonomous driving system and makes judgments to provide autonomous driving appropriate for the environment in which the vehicle is traveling (Fig. 3).

For example, when an old white line is faded or cannot be seen due to snow, the infrastructure-linked autonomous driving system using satellites is mainly used for autonomous driving. On the other hand, when

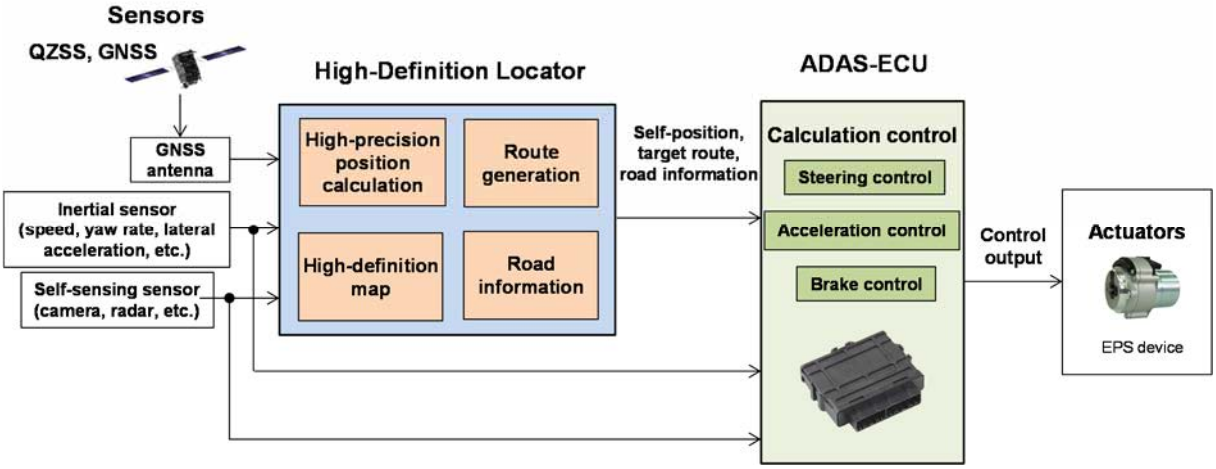

Fig. 2 xAUTO vehicle control system

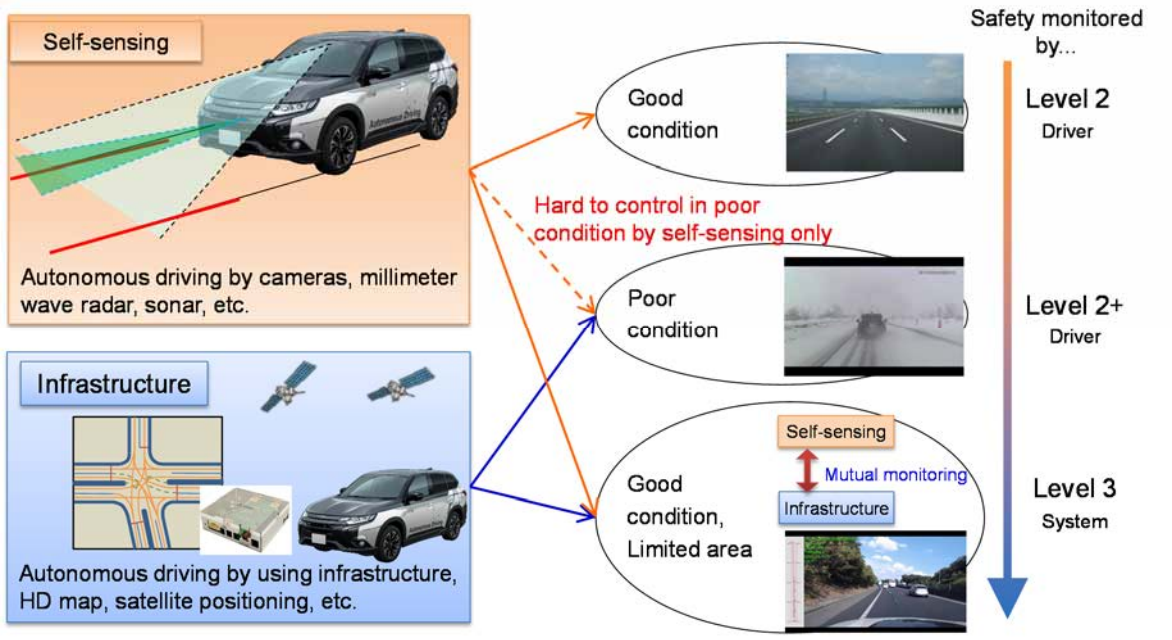

Fig. 3 Combination of autonomous driving technology

satellite signals cannot be received while passing through a tunnel or due to other reasons, the self-sensing system is mainly used for autonomous driving.

6. Demonstration experiments on public roads

A demonstration experiment on public roads using xAUTO and CLAS signals from the QZSS during test operation was conducted for the first time in the world in September 2017. In addition, an autonomous driving experiment using dynamic maps was performed by participating in a SIP's large-scale demonstration experiment and autonomous driving was tested under conditions of poor visibility due to snow and a snowstorm. The feasibility and robustness of the xAUTO's autonomous driving system were verified through these experiments on public roads (Fig. 4).

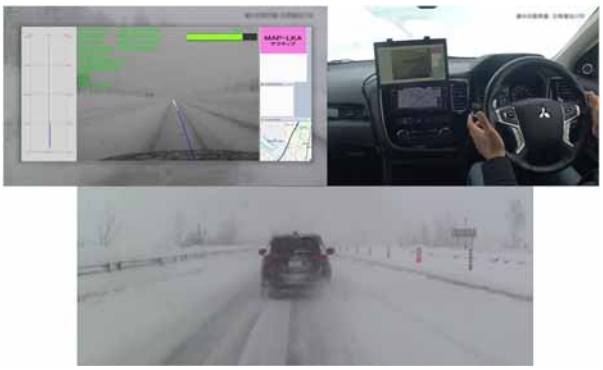

Fig. 4 Field test on a snowy road

Autonomous driving has been tested on roads around the world using the infrastructure-linked and self-sensing autonomous driving systems to verify both safety and comfort in various environments.

Path Planning and Vehicle Control Technologies for Autonomous Driving Systems

Authors: *Tomoki Uno** and *Rin Shinomoto**

To expand the applications of autonomous driving technologies aimed at reducing traffic accidents, technologies to recognize various surrounding environments correctly, and technologies to judge and control that ensure safety and ride comfort in such environments are important. This paper describes path planning technologies that can be applied to complicated environments and vehicle integrated control technologies that ensure highly accurate tracking of paths and comfortable ride.

1. Path Planning Technologies

1.1 Path planning technologies for autonomous driving

Conventional path planning technologies include graph search methods, such as Dijkstra[(1)] and A*,[(2)] and sampling-based planning methods such as rapidly-exploring random tree (RRT).[(3)] These methods enable high-speed path searching in complicated environments. However, because they do not consider the motion characteristics of the vehicle, the planned path causes jerky motion of the vehicle, which degrades the ride comfort. Many path planning technologies that use curves or combine with motion model have been proposed to overcome this problem. Mitsubishi Electric Corporation has been developing PF-RRT, which is a sampling-based path planning technology using a particle filter (PF) in order to realize smooth vehicle behavior and adaptability to complicated environments.[(4), (5)]

1.2 Path planning technologies using PF

PF is a state estimation method that approximates a conditional probability distribution with a group of data called particles. Target of estimation is a virtual vehicle in ideal state. Ideal observation values assumed to be obtained from the virtual vehicle are used to calculate state transition to approach the ideal state from the current state. The ideal state is equal to objectives in path planning, such as follow the center of a target lane and maintaining the target speed and safe distance from surrounding obstacles.

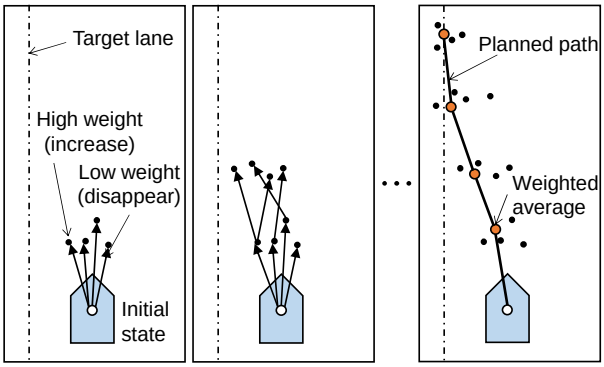

Fig. 1 Conceptual diagram of PF path planner

Figure 1 shows the flow of path planning. First, the states are predicted using a system model for all particles. Random numbers are used as input to the system model to vary the states of the particles. The weight of each particle is calculated based on the difference between the observation value obtained from the state of each particle and the ideal observation value. Resampling (increasing and decreasing of particles) is then performed based on the weight. By repeating the state prediction, weight calculation, and resampling, probability distribution of state at each time is approximately obtained by particles. The average values of the state quantities of the particles are calculated to obtain the path to the ideal state from the current state.

1.3 PF-RRT path planning

To achieve path planning in a complicated environment, Mitsubishi Electric has developed a path planning technology in which PF is combined with input-based RRT, a sampling-based planning method. RRT is a method to expand data group in a tree structure using random numbers and search a path from the data group. In input-based RRT, when a tree is expanded, nodes are randomly selected and branches are extended according to the system model. The nodes are connected based on the motion characteristics represented by the system model. Therefore, a path can be searched considering the motion characteristics of the vehicle.

This section describes the flow of the developed

**Advanced Technology R&D Center*

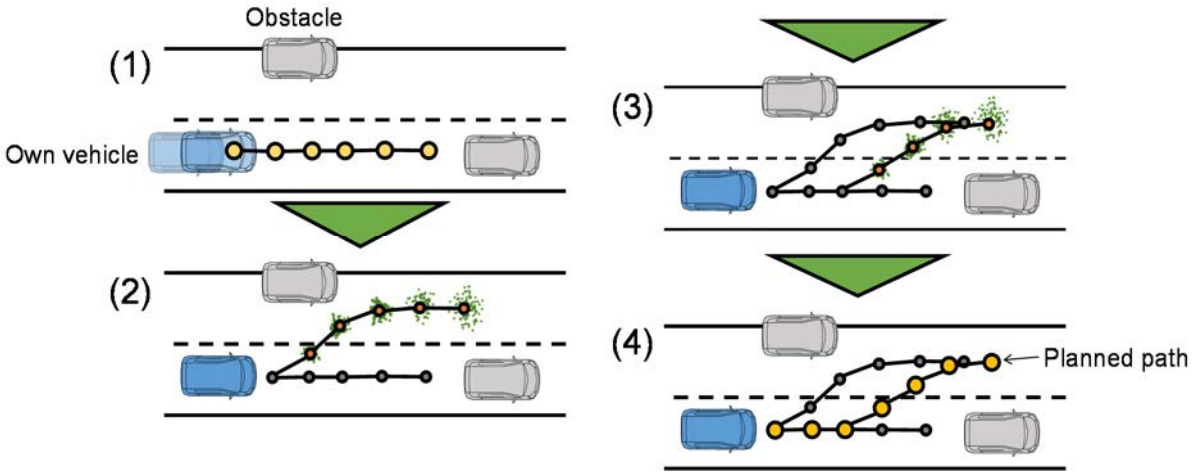

Fig. 2 PF-RRT path planner

path planning technology with reference to Fig. 2. (1) Data group including the position and velocity are held in a tree structure. (2) Randomly selected nodes are used as initial positions to create a path using PF and the created path is added to the tree as a new branch. (3) Step (2) is repeated to expand the tree. (4) The path that minimizes the reaching cost is selected from the tree and output to the controller.

In this way, by expanding a tree with randomness it is possible to search a path in a complicated environment.

2. Vehicle Integrated Control Technologies

2.1 Vehicle control technologies for autonomous driving

Recently, thanks to the improvement of computing power, nonlinear model predictive control (NMPC) has been gaining attention. NMPC is a control theory that solves an optimization problem for a finite time-horizon in the future for each sampling frequency and the initial value of the obtained solution is applied as a control input. Although the calculation loads are high, the theory has various advantages, for example, it can handle multivariable control problems and nonlinear models and constraints can be explicitly considered. Therefore, we have been developing a control system using NMPC that controls integrally the longitudinal and lateral motion of the vehicle, in order to follow the generated path with high accuracy and realize comfortable ride.[6] By using NMPC it is possible to consider the trackability of paths, ride comfort such as acceleration and jerk, and their upper limits.

2.2 Formulation of nonlinear model predictive control

In NMPC, various factors need to be set: a vehicle dynamics model that predicts the states from now to a certain point in the future; a cost function designed such that the vehicle will follow a created path while maintaining ride comfort; and upper and lower limits (constraints) for the state variables and control input. Our study used a vehicle model in which a general bicycle model[7] was combined with a nonlinear tire model using the Pacejka formula.[8] The state variables of the model are longitudinal and lateral positions, yaw angle, longitudinal velocity, lateral velocity, yaw rate, steering angle, front and rear wheel side-slip angles, and front and rear wheel angular velocity. The input variables are steering angular velocity and braking and driving torque of the front and rear wheels. As the cost functions, the trackability was considered using deviation of the self-position from the target path and that of the velocity from the target speed; the ride comfort was considered based on longitudinal acceleration, longitudinal jerk, yaw rate, and steering angular velocity. Constraints were imposed on the location deviation, which was equivalent to the lane width, steering angle, steering angular velocity, and braking and driving torque of the front and rear wheels. The solution for an NMPC controller that was designed as described above is calculated by sequential quadratic programming and the optimal solution is applied to the steering angle and speed to control the vehicle.

3. Verification Using Actual Vehicles

3.1 Configuration of the autonomous driving system

Figure 3 shows the configuration of the autonomous driving system. The system uses a Global Navigation Satellite System (GNSS) and high-definition map. The high-definition map has point cloud information on the latitude and longitude of the center of lanes. The system also has sensors that measure the position and speed of obstacles. The sensor and map information are used to create a target path and speed with PF-RRT. To follow

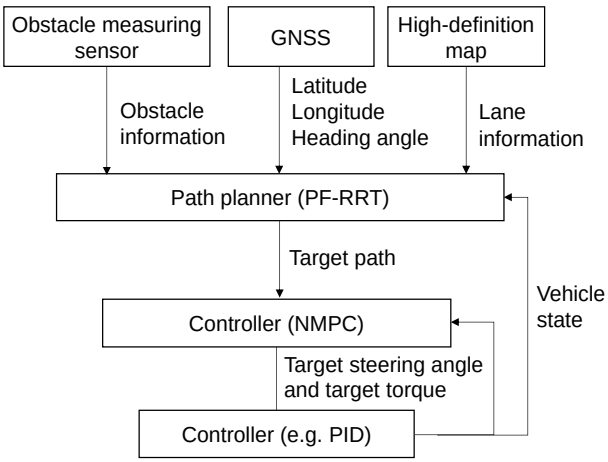

Fig. 3 System configuration

the target path, the NMPC controller calculates the target steering angle and target braking and driving torque. The vehicle controller controls the steering angle and speed so as to follow the calculated target values by the PID control of the like.

3.2 Verification results using an actual vehicle

The effectiveness of this autonomous driving system was checked in a test using an actual vehicle. In the test, the vehicle traveled at the target speed of 80 km/h on a straight two-lane road while avoiding stationary obstacles. Figure 4 shows the vehicle trajectory in the test, and Figure 5 shows the lateral position error, steering angle, and vehicle velocity. Figure 5 shows that the vehicle followed the path with smooth steering while maintaining the target speed of 80 km/h. These results confirm that the autonomous driving system can control the steering and vehicle velocity and can drive a vehicle while changing lanes to avoid obstacles.

4. Conclusion

To popularize the path planning and vehicle control technologies described in this paper, it is important to enhance the robustness and reduce the calculation cost, in addition to applying them to more complicated cases. Mitsubishi Electric has been working to solve these issues, aiming to establish practical autonomous driving technologies.

5. References

(1) E. W. Dijkstra: A note on two problems in connection with graphs, Numerische mathematik, Vol. 1, No. 1, pp. 269–271 (1959).
(2) P. E. Hart, N. J. Nilsson, and B. Raphael: A formal basis for the heuristic determination of minimum cost paths, IEEE Trans. on Systems Science and Cybernetics, Vol. 4, No. 2, pp. 100–107 (1968).
(3) S. M. LaValle: Rapidly-exploring random trees: A new tool for path planning (1998).
(4) K. Berntorp and S. D. Cariano: Particle filtering for online motion planning with task specifications, American Control Conference, pp. 2123–2128 (2016).
(5) R. Shinomoto, et al.: Path Planning using Particle Filter for Autonomous Driving, 2018 JSAE Congress (Autumn), Proceedings, No. 163-18 (2018).
(6) T. Uno, et al.: Vehicle Integrated Control by Nonlinear Model Predictive Control in RTK-GPS Based Autonomous Driving System, 2018 JSAE Congress (Autumn), Proceedings, No. 163-275 (2018).
(7) K. Berntorp, B. Olofsson, K. Lundahl, and L. Nielsen: Models and methodology for optimal trajectory generation in safety-critical road-vehicle manoeuvres, Vehicle System Dynamics, Vol. 52, pp. 1304–1332 (2014).
(8) H. Pacejka: Tire and Vehicle Dynamics, Third Edition, Butterworth-Heinemann (2012).

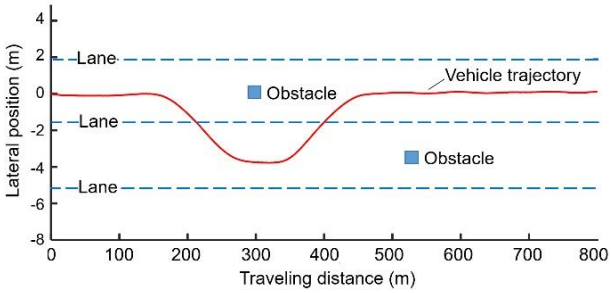

Fig. 4 Vehicle trajectory to avoid obstacles

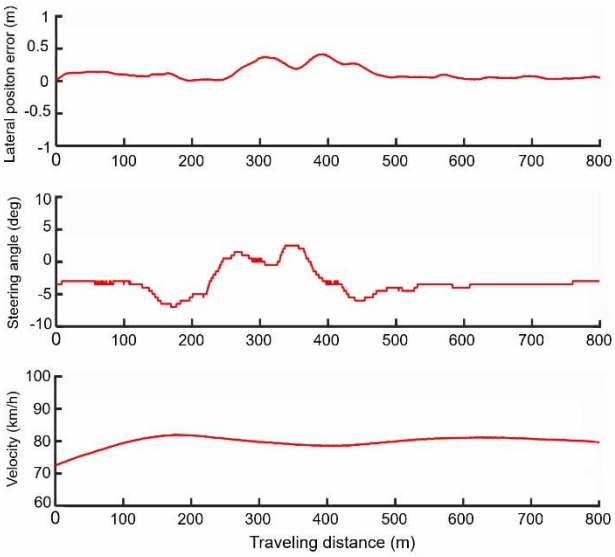

Fig. 5 Vehicle states when avoiding obstacles

In-vehicle Monitoring System

Author: *Taro Kumagai**

In order to determine the conditions of occupants in vehicles and improve their safety and comfort, Mitsubishi Electric Corporation has been developing an in-vehicle monitoring system (IMS). This paper describes the characteristics, functions, and robustness of our IMS (Fig. 1).

1. Characteristics of IMS

Our IMS, with a wide-angle camera installed at the center of the dashboard as shown in Fig. 2, can monitor the driver and person in the passenger seat at the same time. In addition, since it captures images over a wide range in the vertical direction in addition to the horizontal direction, it can detect the shoulders and hands in addition to the face. Therefore, the IMS's functions can be easily expanded, unlike driver monitoring systems that only capture images of the driver's face with high accuracy for monitoring.

2. IMS's Functions

The IMS's functions are broadly divided into a sensing function that detects faces and outputs basic information such as head pose, eye opening rate, gaze direction, and shape of a hand, and an application function that uses the information detected by the sensing function to judge whether there is an occupant and to detect looking-aside, drowsiness, and gestures.

The two functions of the IMS are described in detail below.

Fig. 1 Sensing image

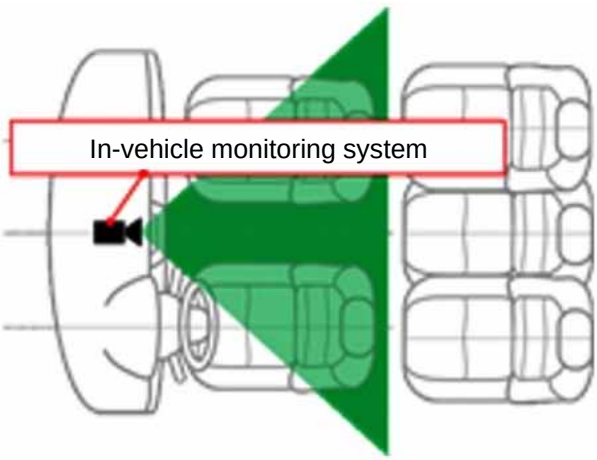

Fig. 2 Mounting position and imaging range

*Sanda Works

2.1 Looking-aside detection function

Figure 3 illustrates the processing flow of the looking-aside detection function. Our IMS first detects the face and parts and uses the information to detect the head pose. The function determines that the driver is looking aside when the head pose exceeds the threshold, which can be changed based on vehicle information. This helps prevent misdetection of looking-aside when the vehicle is not traveling and when it is turning. The function also assists the driver by, for example, issuing a warning at a more appropriate time in more appropriate conditions when the effective field of view is narrower when driving at high speed.

To detect looking-aside, in addition to using head pose and vehicle information as shown in Fig. 3, our IMS can also use gaze direction and the results of monitoring the outside of the vehicle. For these additional factors, detection procedures need to be determined considering the increased risk of misdetection due to increased indexes, complexity of evaluation, and higher dependence on other systems.

2.2 Drowsiness detection function

Our IMS uses percent of eyelid closure (PERCLOS) to detect drowsiness. PERCLOS, which refers to the percent of closed eyes per unit time, is thought to correlate well with level of drowsiness and show little variation among individuals.(1)

To detect drowsiness, changes in expressions and posture, gestures, and other similar information may be used in addition to PERCLOS. Especially, our IMS is the only system that can detect drowsiness using changes in posture and gestures since its wide-angle camera can also monitor the trunk below the shoulders and a wide area to both sides.

3. Robustness

An onboard IMS for mass production must be robust and the limitations of its monitoring and application functions or performance should be understood, since it will be used by various users under diverse environments. For our IMS, we have selected four main perspectives for ensuring robustness and understanding performance limitations: environmental robustness, individual difference robustness, accessory robustness, and behavior robustness.

Environmental robustness refers to items of robustness to various types of onboard environments. Many of such items are related to light such as artificial light and sunlight (Fig. 4). Individual difference robustness refers to the robustness of the IMS to changes for each individual and among individuals. Accessory robustness refers to robustness to wearing articles such as glasses, sunglasses, and face masks as shown in Fig. 5 in the case of faces. Behavior robustness refers to robustness to the behavior of an occupant during driving, for example, covering part of the face with a hand and changes in expressions and posture.

In developing our IMS, we have listed detailed items for verifying robustness and have linked verification databases to the items. We are repeatedly conducting evaluations and improvements using the databases to improve the quality to a sufficient level for mass production and installation on vehicles.

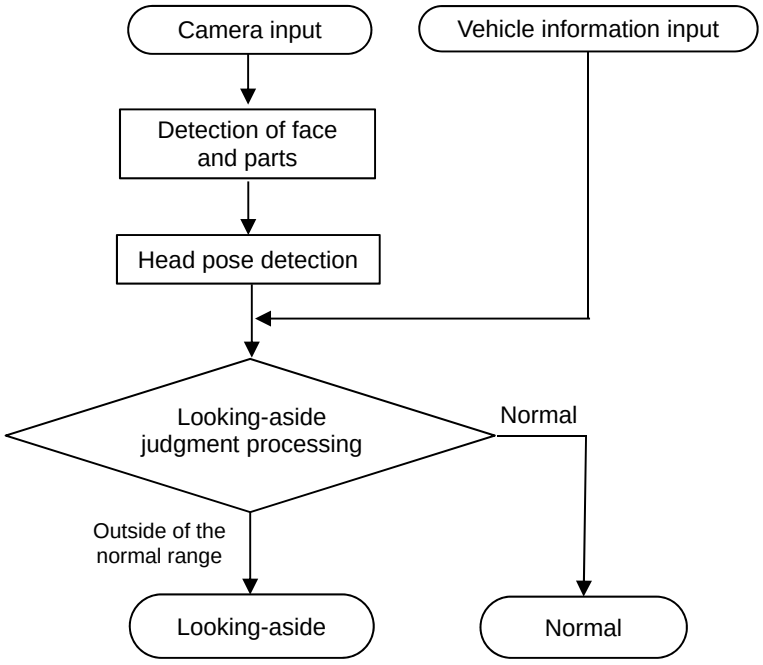

Fig. 3 Processing flow of looking-aside detection

Fig. 4 Example of external light contrast on the face

Fig. 5 Various accessories worn on the face

4. Conclusion

This paper described the characteristics of our IMS and the concepts of robustness. We will develop functions for the IMS that monitors occupants of seats other than the front seats to contribute to enhancing safety.

5. Reference

(1) R. Knipling, “Perclos: A valid psychophysiological measure of alertness as assessed by psychomotor vigilance”, 1988.

4GL-IPU: Power Unit for 2-Motor System

Authors: *Satoshi Ishibashi** and *Noriyuki Wada**

Mitsubishi Electric Corporation first commercialized Intelligent Power Modules (IPM) for hybrid electric vehicles in 1997. Since then, we have been contributing to the electrification of vehicles by releasing products such as 4GS-Integrated intelligent Power Unit (4GS-IPU) with heat sink and motor control functions as a result of our effort to downsize IPM, increase the output power, and integrate the functions. Our newly developed 4GL-IPU described in this article is for the high-power 2-motor systems, which enables motor-driven travel even in a high-speed region and in full acceleration. (Fig. 1).

1. Characteristics of the 4GL-IPU

4GL-IPU has two high-power inverters: one for the high-power traction motor and the other for the generator motor that supplies high power to the traction motor. It also has a voltage boost-up converter that boosts the voltage of the main battery and an insulated step-down converter that lowers the voltage of the main battery to 12 V for the auxiliary battery (Fig. 2).

To realize 4GL-IPU, four requirements needed to be satisfied at the same time: higher power of the two inverters; higher functionality by integrating the voltage boost-up converter and the step-down converter;

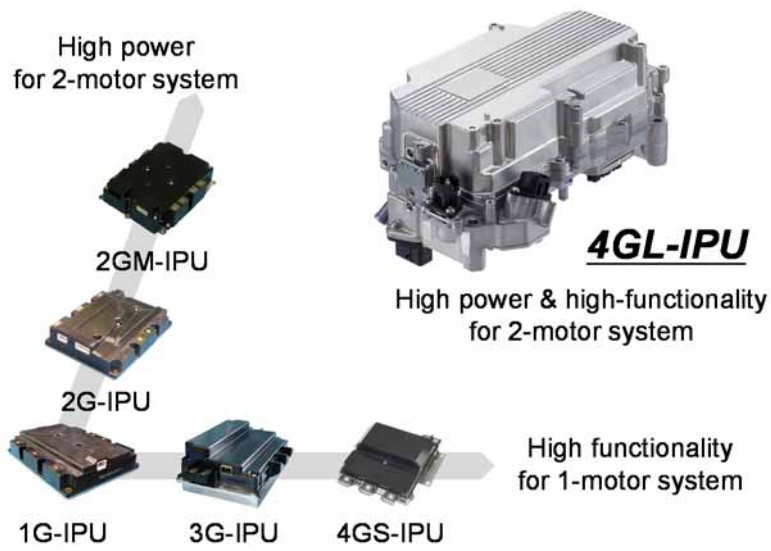

Fig. 1 Evolution of IPU and 4GL-IPU

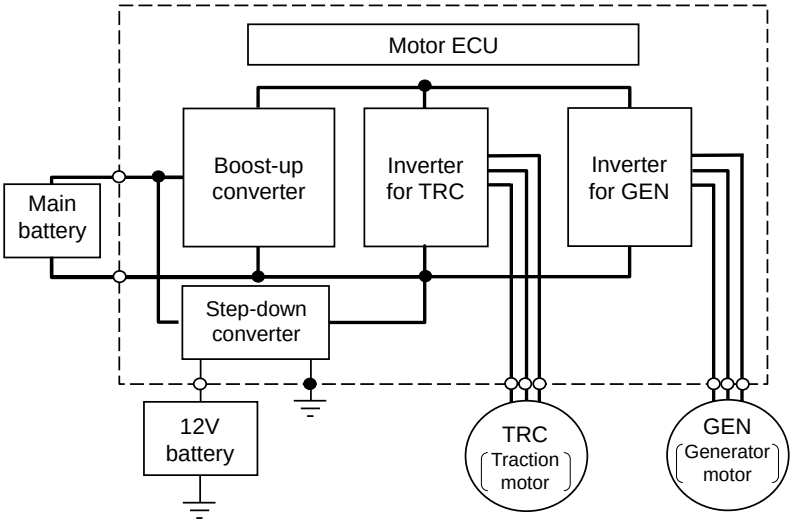

Fig. 2 Block diagram of 4GL-IPU

*Himeji Works

downsizing to allow 4GL-IPU to be installed in the engine compartments of various models; and high vibration resistance to allow IPU to be directly mounted in the transmission. To achieve these requirements, the loss in the power devices, which are main heat sources, was reduced and the heat radiation was enhanced. In addition, heat-producing parts, such as the power module and voltage boost-up reactor, were closely mounted on both sides of a highly-rigid water cooling heat sink to shorten the wiring length between the parts while considering their heating (Fig. 3).

2. Technologies Applied to the 4GL-IPU

To effectively achieve the aforementioned higher power, higher functionality, downsizing, and high vibration resistance, various technologies were applied to 4GL-IPU, which include the cutting-edge low-loss power device, low-loss motor control, a new type of power module and heat radiation structure, and a voltage boost-up converter with our unique circuit system.

2.1 Power device and motor control

The power of traction motors driven by 4GL-IPU is approximately five times that of motors for 1-motor hybrid electric vehicles driven by our conventional models (e.g., 4GS-IPU). When the power of the generator motor is included, the total power of 4GL-IPU is approximately ten times that of our conventional model. To reduce the size without sacrificing efficiency, it is particularly important to reduce the loss. The power device adopts the latest seventh-generation Insulated Gate Bipolar Transistor (IGBT) and Relaxed Field of Cathode (RFC) diode to reduce the conduction loss.

However, in the high-power range, the system voltage (applied voltage) increased to approximately four times that of the conventional system due to the boosting. As the switching loss is proportional to the applied voltage and carrier frequency, for reducing the loss, it is essential to reduce the carrier frequency. In addition, the motor rotation speed increased to approximately twice that of the conventional model. At higher rotation speed, the fundamental frequency is higher and the number of switching per cycle of the electric angle decreases, which impairs the controllability. To retain controllability, the carrier frequency needs to be set higher in line with the increased rotation speed in the case of asynchronous Pulse Width Modulation (PWM) used for the conventional models. In other words, it is difficult to increase the motor rotation speed (increase the fundamental frequency) and reduce the switching loss (reduce the carrier frequency) at the same time.

Therefore, synchronous PWM, which was used in our motor control for electric trains, was realized using commercially available general-purpose micro-computers for the first time. In synchronous PWM, even at high rotation speed, the pulse number can be made uniform, thus enhancing controllability. For 4GL-IPU, asynchronous PWM and synchronous PWM coexist and the carrier frequency is finely switched based on the motor rotation speed, which reduces the switching loss by reducing the carrier frequency and realizes controllability to cope with sudden torque changes in the

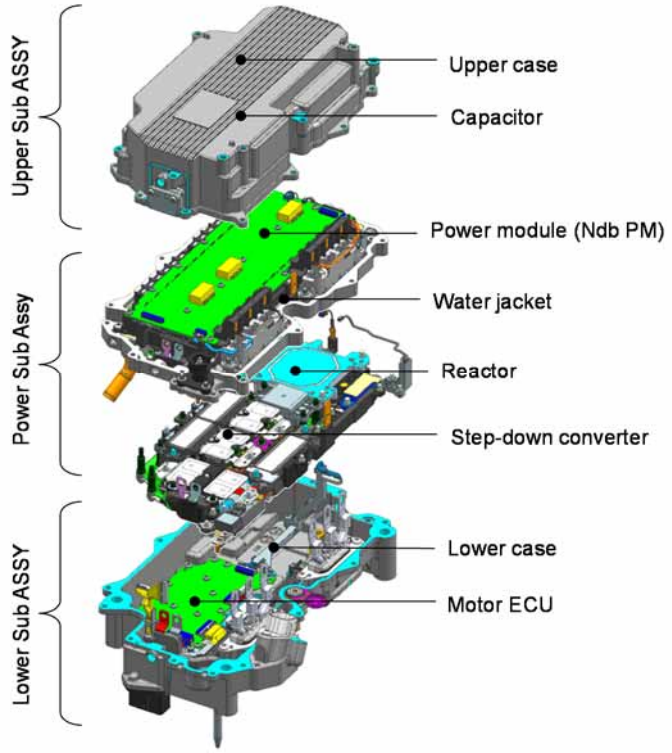

Fig. 3 Parts layout of 4GL-IPU

high-speed range, which is difficult with the conventional method (Fig. 4).

2.2 New heat radiation structure and water sealing structure

To fit the high-power inverters and voltage boost-up converter into a small housing, we developed new Nano sinter die-bonded Power Module (NdbPM) with high heat radiation and highly-rigid heat sinks in a compact water sealing structure.

The Transfer molded-Power Module (T-PM) used for the conventional model was for 1-motor hybrid electric vehicles, where the main task was torque assistance for a short time, and for 2-motor hybrid electric vehicles, for which the output was relatively small. Therefore, the heat radiation structure was designed to reduce the transient thermal resistance in order to supply large currents for a short time. On the other hand, the heat radiation structure of NdbPM is designed to reduce the constant thermal resistance in order to pass large currents continuously. Specifically, the insulating material was changed to ceramic base plates from resin sheets and the die bond of the power device was changed to sinter die-bonding with Ag nano-particles from solder in order to enhance the thermal conductivity of the heat radiation paths, reduce the thickness, and eliminate voids.

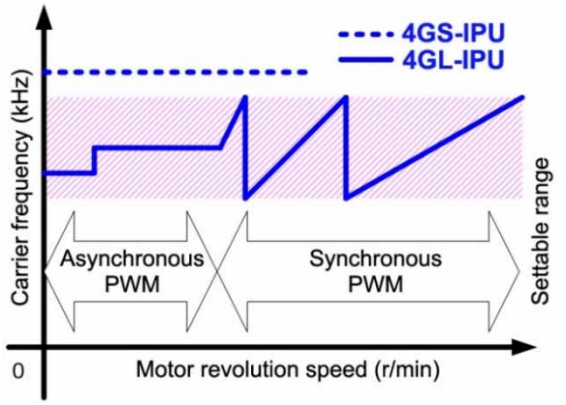

Fig. 4 Comparison of PWM operation mode

In the conventional model, the T-PM is secured to the water cooling heat sink with a spring and screw via thermal grease. In 4GL-IPU, NdbPM is directly soldered to the heat sink to reduce the size by eliminating fixing materials and also to improve the heat radiation. In addition, for the conventional model, the water sealing between the water cooling heat sink and water jacket is realized by using sealing materials (e.g., O-rings) and by fastening with multipoint screws. In 4GL-IPU, the circumference and the center of the water path are connected by Friction Stir Welding (FSW). This method eliminates sealing materials and fastening with screws, and also makes it possible to firmly connect the water cooling heat sink to the thick water jacket, which forms the case, in a line instead of points. Since the water cooling heat sink is the base of various parts, the firm connection of the water jacket and water cooling heat sink by FSW simultaneously solves various issues, including securing high vibration resistance required to install the modules directly onto transmissions, higher reliability of the water sealing thanks to the elimination of sealing materials, and downsizing due to the elimination of O-rings and multipoint screwing, which requires floor area. These improvements have made it possible to install a power module required for two high-power inverters and a voltage boost-up converter on the limited floor area of a heat sink in a simple planar layout (Fig. 5).

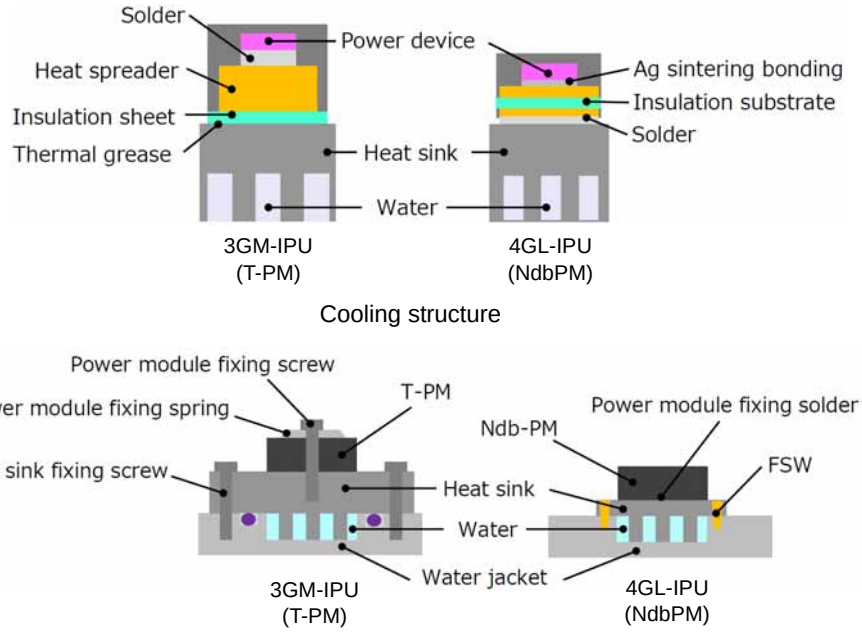

Fig. 5 Comparison of cooling and sealing structure

2.3 Voltage boost-up converter using our unique circuit system

The higher voltage achieved by using the voltage boost-up converter reduces the size thanks to higher efficiency of the motor inverter and smaller currents. However, the voltage boost-up converter requires new parts such as a power module, reactor, and smoothing capacitor.

Generally, a higher switching frequency of a power device enables the reactor to be downsized. On the contrary, the higher the frequency of a power device, the greater the switching loss. To solve this problem, we adopted a new circuit system in place of the common boost chopper method. Our unique circuit system has a flying capacitor (C0) and repeats the four modes shown in Fig. 6 to raise the voltage. This method doubles the reactor frequency without increasing the switching frequency of the power device. The method allowed us to reduce the size of the reactor by approximately 40% compared to the conventional method without increasing the switching loss for the power device.

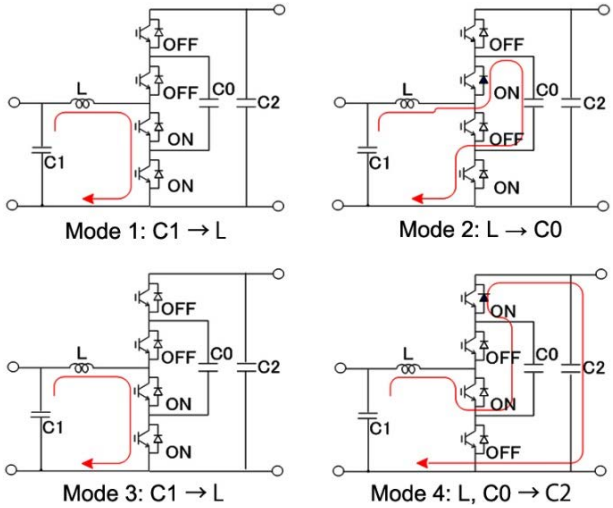

Fig. 6 Operation mode of Mitsubishi's original boost converter

These improvements allowed us to downsize the reactor and install a low-profile step-down converter on the back of the water cooling heat sink. Step-down converters used to be installed in the interior of vehicles. Integrating such converters into 4GL-IPU to be installed in the engine compartment enlarges the space within the vehicle and the luggage compartment.

3. Conclusion

Mitsubishi Electric has been developing smaller and lighter IPU with higher power and integrated functions and putting them on the market since the appearance of electric motor vehicles. Based on the concepts of the existing IPU that are used in many models, small and high-functionality 4GL-IPU with high power were developed by combining the latest inhouse-produced power devices, control methods used in other sectors, new connection techniques, our unique booster circuit system, and other technologies.

4GL-IPU enable vehicles to be driven on high-power motors, thus improving environmental performance, which has become increasingly important in recent years, while making driving more fun. They have also enlarged the space in vehicles by relocating the step-down converters from the interior of the vehicle to the engine compartment. We will continue to develop products that satisfy contradictory market needs for smaller and lighter products and for higher power and functionality, thus contributing to the spread of electric motor vehicles and countermeasures against global warming.

4. References

(1) Ishibashi, S., et al., "4GL-IPU: Power Unit for 2 Motor System," Mitsubishi Denki Giho, 93, No. 5, 2019.
(2) Michinaka, T., et al., "Third-Generation Power Unit for HEVs," Mitsubishi Electric ADVANCE, Dec. 2010.
(3) Hino, Y., et al. "Packaging Technologies for High Temperature Power Semiconductor Modules," Mitsubishi Electric ADVANCE, Mar. 2015.
(4) Kamibaba, R., et al., "7th Generation Power Chip Technologies for Industrial Application," Mitsubishi Electric ADVANCE, Sep. 2016.

Electromagnetic Design of Electric Motor for Crankshaft-mounted Integrated Starter-Generator System of 48V Hybrid Vehicles

Authors: *Junji Kitao** and *Masatsugu Nakano***

Recently, electric vehicles (EVs) and hybrid electric vehicles (HEVs) have been rapidly spreading in the automobile market for reducing CO_2 emissions. In line with this trend, Mitsubishi Electric Corporation has developed and released a small and lightweight high-efficiency crankshaft-mounted 48V-integrated starter-generator (ISG) system for mild-HEVs. This paper describes the characteristics of this system and the electromagnetic design of electric motors.

1. Characteristics of the Crankshaft-Mounted 48V-ISG System

1.1 Outline of the crankshaft-mounted 48V-ISG system

Figure 1 illustrates the configuration of this system. As the structure of this system, an electric motor is installed between the engine and transmission. The electric motor rotor is directly connected to the crankshaft, which enables the driving force of the electric motor to be directly transmitted, resulting in high torque transmission and shorter response time of the torque. However, the magnetic circuit needs to be formed in a thin, flat, and cylindrical limited space due to the layout restrictions of the engine room and for weight reduction.

1.2 Outline of electric motors for the 48V-ISG system

HEVs powered by engines and electric motors are broadly divided into full-HEVs and mild-HEVs depending on the functions. Full-HEVs can drive only on the electric motor with the engine stopped, which is expected to significantly improve the fuel economy. On the other hand, mild-HEVs do not drive only on the electric motor, and have a torque assist and other functions for energy regeneration from decelerating vehicles. Mild-HEVs are characterized by a simple system. The total cost of 48V mild-HEVs in particular is lower compared to high-voltage systems and they are expected to spread more rapidly.

The 48V-ISG system for mild-HEVs can improve the fuel economy by performing restart of the engine, energy regeneration from the decelerating vehicle, and torque assist under acceleration. Figure 2 shows our 48V-ISG system. The electric motor is thin and flat and the inverter is mounted to the electric motor housing.

2. Electromagnetic Design of Electric Motors for the 48V-ISG System

2.1 Performance requirements

Figure 3 shows the performance requirements for electric motors for the 48V-ISG system. To restart an engine, high torque is required in the low-speed range. For torque assist under acceleration, the efficiency needs to be higher in the low-torque range from the low- to medium-speed ranges for higher fuel economy. During energy regeneration from decelerating vehicles, high power regeneration from the low- to medium-

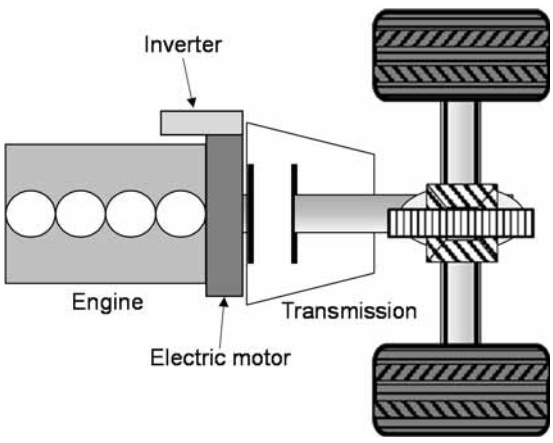

Fig. 1 Engine crankshaft direct-driven system

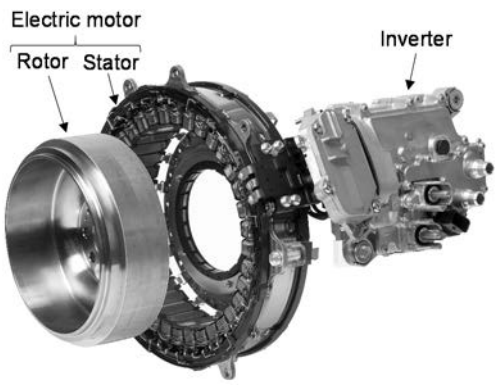

Fig. 2 Crankshaft ISG system for 48V hybrid

*Advanced Technology R&D Center **Himeji Works

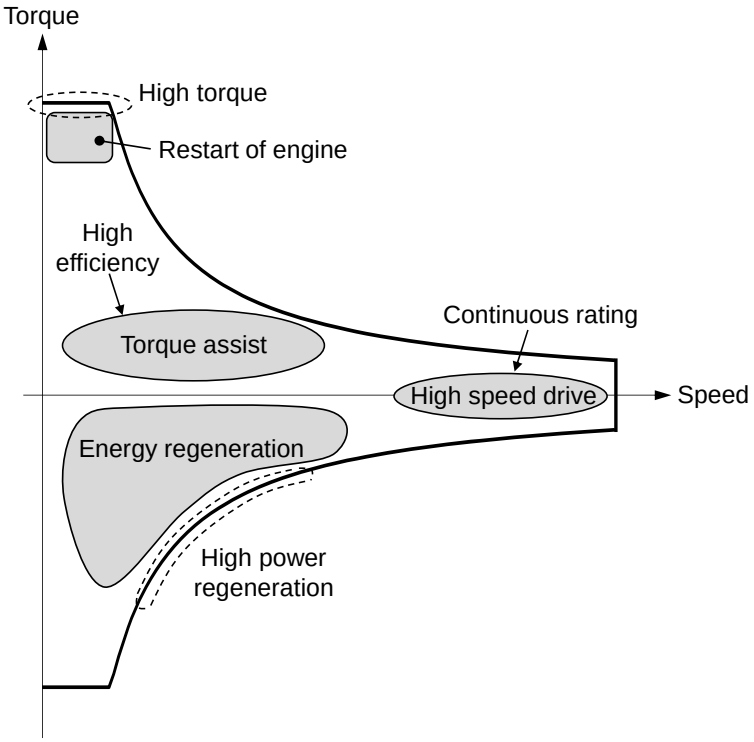

Fig. 3 Performance requirements for electric motor of 48V ISG system

speed ranges is required. In addition, since the engine power is transmitted via the rotor in this system, the system needs to function throughout the entire operation range of the engine and continuous rating is required even in the high-speed range. Thus, the system requires high torque and high power regeneration and must also be highly efficient in the low-torque range from the low- to medium-speed ranges. Therefore, the system uses permanent magnet synchronous motors for a motor system since such motors deliver high torque and high power regeneration. However, to enable continuous rating of a permanent magnet synchronous motor to the maximum engine speed at a low voltage of 48 V, current needs to be supplied to decrease the induced electromotive force (magnetic flux-weakening control). Therefore, reducing the current for performing magnetic flux-weakening control is a key point in the electromagnetic design of this system.

2.2 Consideration of the winding structure

The winding structure of electric motors is broadly divided into concentrated winding where a coil is formed around one tooth and distributed winding where a coil is formed around multiple teeth. This section describes the appropriate winding structure for electric motors for the 48V-ISG system.

Figure 4 shows the electromagnetic field analysis results of systems with each winding structure. The short-time rating in Fig. 4(a) shows the speed-torque characteristic at the maximum current. The continuous rating in Fig. 4(a) shows the speed-torque characteristic at the same current density supposing continuous rating. The figure shows that the short-time rating on the distributed winding is higher than that of the concentrated winding at any speed. The reluctance torque on the distributed winding is higher than that on the concentrated winding and as a result, the distributed winding can realize high torque and high power. However, in terms of the continuous rating, the torque is higher on the concentrated winding in the medium- to high-speed ranges. This is because the current for performing magnetic flux-weakening control could be reduced. This result is also seen in the efficiency characteristics in Fig. 4(b) and 4(c). On the concentrated winding, the high efficiency range could be enlarged to the high-speed range by reducing the copper loss due to the current for performing the magnetic flux-weakening control.

2.3 Consideration of increasing number of pole pairs

Adopting concentrated winding can shorten the coil end. In addition, increasing number of pole pairs can further reduce the height of the coil end and the area of the iron core necessary for forming a magnetic circuit. Therefore, to satisfy the performance requirements in a limited space like in this system, it may be effective to use the concentrated winding and increasing number of pole pairs. However, since increasing number of pole pairs increase the electrical angular frequency of electric

motors, the increase in iron loss is of concern. Since the number of poles is thus an important parameter in the electromagnetic design, this section describes the relationship between the performance requirements and number of poles.

Figure 5 shows the electromagnetic field analysis results of the maximum torque and maximum generated power electric motors having different numbers of poles. The maximum torque shown in Fig. 5(a) increased due to the increasing number of pole pairs. However, the figure shows that when the number of poles reaches a certain number, the maximum torque no longer increases even when the number of poles is increased. Since increasing number of pole pairs can reduce the area of the iron core forming a magnetic circuit necessary for electric motors, the torque can be increased by relieving the magnetic saturation of each part and enlarging the rotor diameter. Meanwhile, increasing number of pole pairs increase the number of slots and thereby the leakage magnetic flux between the slots of the stator also increases. This trade-off results in the trend as shown in Fig. 5(a). Figure 5(b) shows that the maximum generated power is lower when the number of poles is large. As mentioned previously,

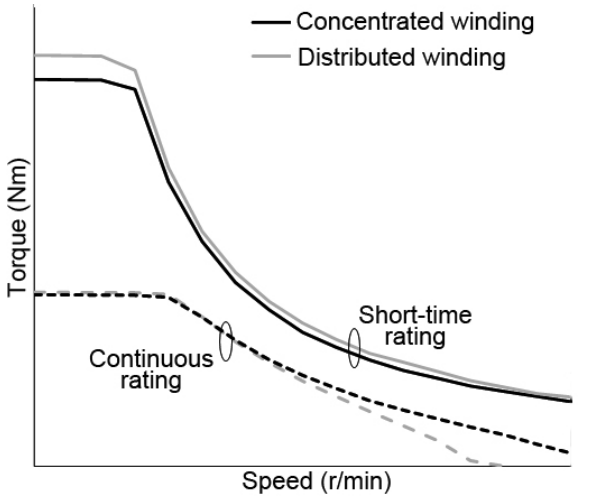

(a) Short-time rating and continuous rating

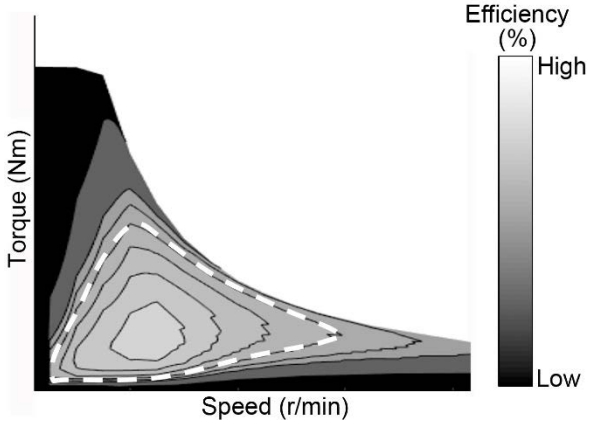

(b) Efficiency characteristics of concentrated winding

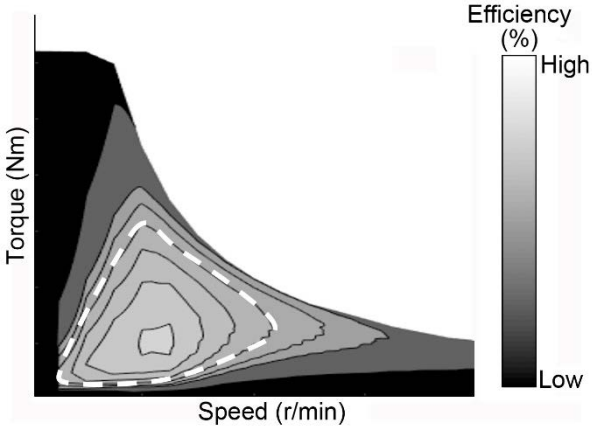

(c) Efficiency characteristics of distributed winding

Fig. 4 Comparison between concentrated winding and distributed winding

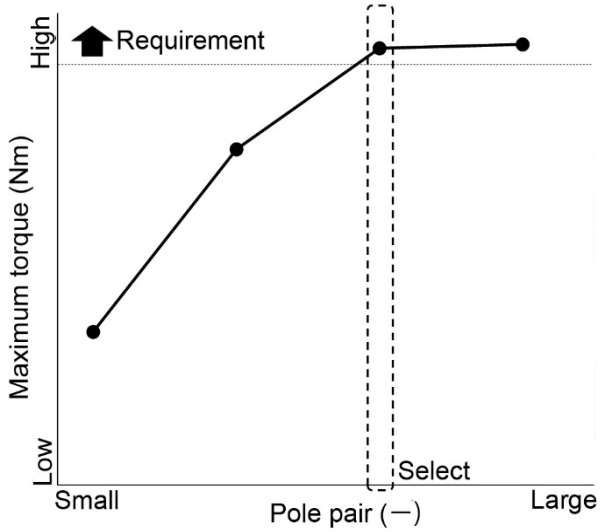

(a) Maximum torque

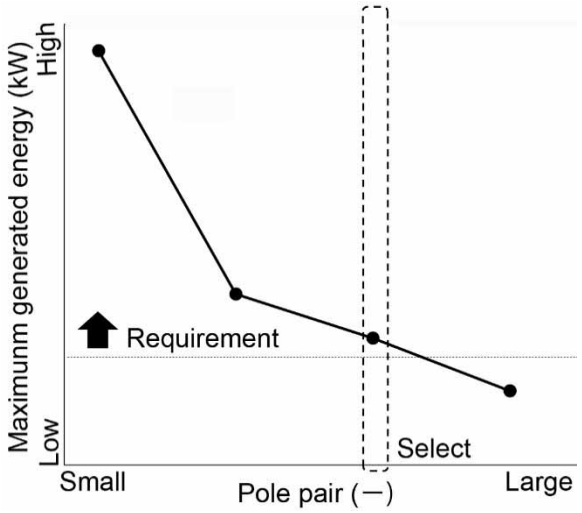

(b) Maximum generated power

Fig. 5 Maximum torque and maximum generated power

increasing number of pole pairs increase the leakage magnetic flux between slots, so the inductance increases and as a result, the maximum generated power tends to decrease. Thus, the maximum torque and maximum generated power have a trade-off relationship with the number of poles. Therefore, this system uses the optimum number of poles that satisfies all the performance requirements.

3. Conclusion

This paper described the characteristics of the crankshaft-mounted 48V-ISG system and the electromagnetic design of the electric motors. In the electric motors for the 48V-ISG system, the current for performing magnetic flux-weakening control greatly affects the continuous rating and efficiency characteristics. Therefore, this system uses concentrated winding with increasing number of pole pairs, resulting in the 48V-ISG system that satisfies all the requirements over a wide operation range. We will continue to develop technologies to further reduce the size and weight and increase the power.

MITSUBISHI ELECTRIC CORPORATION